



Water Resources Research

RESEARCH ARTICLE

10.1029/2017WR021876

Key Points:

- We applied a three-dimensional ecosystem model to simulate physical, chemical, and biological dynamics in a large shallow lake
- We found that spatially dependent water residence time represents lake flushing better than traditional flushing time
- Water age influences the spatial and temporal distribution of nutrient retention, primary production, and algal biomass distribution

Supporting Information:

- Supporting Information S1

Correspondence to:

S. A. Bocaniov,
sbocaniov@uwaterloo.ca

Citation:

Bocaniov, S. A., & Scavia, D. (2018). Nutrient Loss Rates in Relation to Transport Time Scales in a Large Shallow Lake (Lake St. Clair, USA—Canada): Insights From a Three-Dimensional Model. *Water Resources Research*, 54, 3825–3840. <https://doi.org/10.1029/2017WR021876>.

Received 16 SEP 2017

Accepted 5 APR 2018

Accepted article online 21 APR 2018

Published online 7 JUN 2018

Nutrient Loss Rates in Relation to Transport Time Scales in a Large Shallow Lake (Lake St. Clair, USA—Canada): Insights From a Three-Dimensional Model

Sergei A. Bocaniov^{1,2}  and Donald Scavia³

¹Graham Sustainability Institute, University of Michigan, Ann Arbor, MI, USA, ²Now at Department of Earth and Environmental Sciences, University of Waterloo, Waterloo, ON, Canada, ³School for Environment and Sustainability, University of Michigan, Ann Arbor, MI, USA

Abstract A nutrient mass balance and a three-dimensional, coupled hydrodynamic-ecological model, calibrated and validated for Lake St. Clair with observations from 2009 and 2010, were integrated to estimate monthly lake-scale nutrient loss rates, and to calculate 3 monthly transport time scales: flushing time, water age, and water residence time. While nutrient loss rates had statistically significant relationships with all transport time scale measures, water age had the strongest explanatory power, with water age and nutrient loss rates both smaller in spring and fall and larger in summer. We show that Lake St. Clair is seasonally divided into two discrete regions of contrasting water age and productivity. The north-western region is dominated by oligotrophic waters from the St. Clair River, and south-eastern region is dominated by the nutrient enriched, more productive waters from the Thames-Sydenham River complex. The spatial and temporal variations in local transport scales and nutrient loss rates, coupled with strong seasonal variations in discharge and nutrient loads from the major tributaries, suggest the need for different load reduction strategies for different tributaries.

1. Introduction

Nutrient dynamics in aquatic systems are driven by interactions among external loads, hydrodynamics, and biogeochemical processes. Previous studies have shown that, at whole system scales, phosphorus (P) and nitrogen (N) loss rates in lakes and estuaries are influenced strongly by water retention times (e.g., Brett & Benjamin, 2008; Nixon et al., 1996; Scavia & Liu, 2009), and can vary seasonally (Dillon & Molot, 1996; Schindler et al., 1973). However, we hypothesize that water retention and associated nutrient loss rates are significantly different when accounting for their spatial and temporal (seasonal) variability, and this helps explain variability in primary production, nutrient loss, and export from the system. However, testing this requires high-resolution measurements of water transport and nutrient dynamics. Unfortunately, the required physical and biological processes, and their interactions, are difficult to measure at such small spatial and temporal scales. This is especially true for large shallow systems that are wind-driven with short flushing times, and where physical and biological processes operate on similar time scales (Sterner et al., 2017). Because large shallow systems are heterogeneous at relatively small spatial scales, it is also difficult to interpolate and extrapolate limited in situ observations. Models can help.

Our objective is to use a three-dimensional hydrodynamic-ecological model of Lake St. Clair (US/Canada) to explore the relationship between nutrient loss rates and variation in transport time and space scales. Lake St. Clair's watershed is one of the most densely populated in the Laurentian Great Lakes, and this binational lake is an important source of drinking water, commercial and sport fishing, and other forms of recreation. Because of its location, it is also a potential source or sink of P load to Lake Erie, which has been the subject of considerable recent attention due to a resurgence of its eutrophication symptoms (Scavia et al., 2014). There is also strong evidence that Lake Erie's harmful algal bloom and hypoxia responses to nutrient loads are influenced by both the form and timing of the P load (Bertani et al., 2016; Bocaniov et al., 2016; Obenour et al., 2014; Rucinski et al., 2016; Scavia et al., 2016). So, it is important to understand how Lake St. Clair modulates loads from the upper Great Lakes and its proximate watershed.

We used the numerical model to test the hypothesis that the timing of Lake St. Clair's productivity and P loss rates are related to the seasonal and spatial dynamics in transport time scales ranging from the annual lake scale to monthly sub-lake scales.

2. Materials and Methods

2.1. Long-Term Monthly Mean Discharges for the Three Largest Tributaries

While water and nutrient fluxes from all tributaries were used in the model analyses and simulations, we also explored the long-term mean daily river discharge for the three largest tributaries to understand their relative influences on seasonal dynamics (St. Clair, Thames, Clinton; Figure 1). These data were based on measurements at Port Huron (United States Geological Survey—USGS station 04159130; <http://tinyurl.com/yph4zwj>; accessed date 14 January 2017) for the St. Clair River, at Thamesville (Water Survey of Canada—WSC station 02GE003; <http://tinyurl.com/y6uxhqoo>; accessed date 14 January 2017) for the Thames, and at the Moravian Drive at Mt. Clemens (USGS station 04165500; <http://tinyurl.com/ybvt8fzf>; accessed date 14 January 2017) for the Clinton River. Long-term mean daily and monthly discharges for the Thames and Clinton Rivers were averaged from 2000 to 2016. Estimates for the St. Clair River were averaged over the past 8 years (2009–2016), the period of record.

2.2. The Model

We used a three-dimensional (3-D) coupled hydrodynamic and ecological model consisting of the Estuary, Lake and Coastal Ocean Model (ELCOM) and the Computational Aquatic Ecosystem Dynamic Model (CAE-DYM). ELCOM is a 3-D hydrodynamic model that simulates the effects of inflows, outflows, atmospheric forcing, and Earth rotation (Hodges & Dallimore, 2014; Hodges et al., 2000), and serves as the hydrodynamic

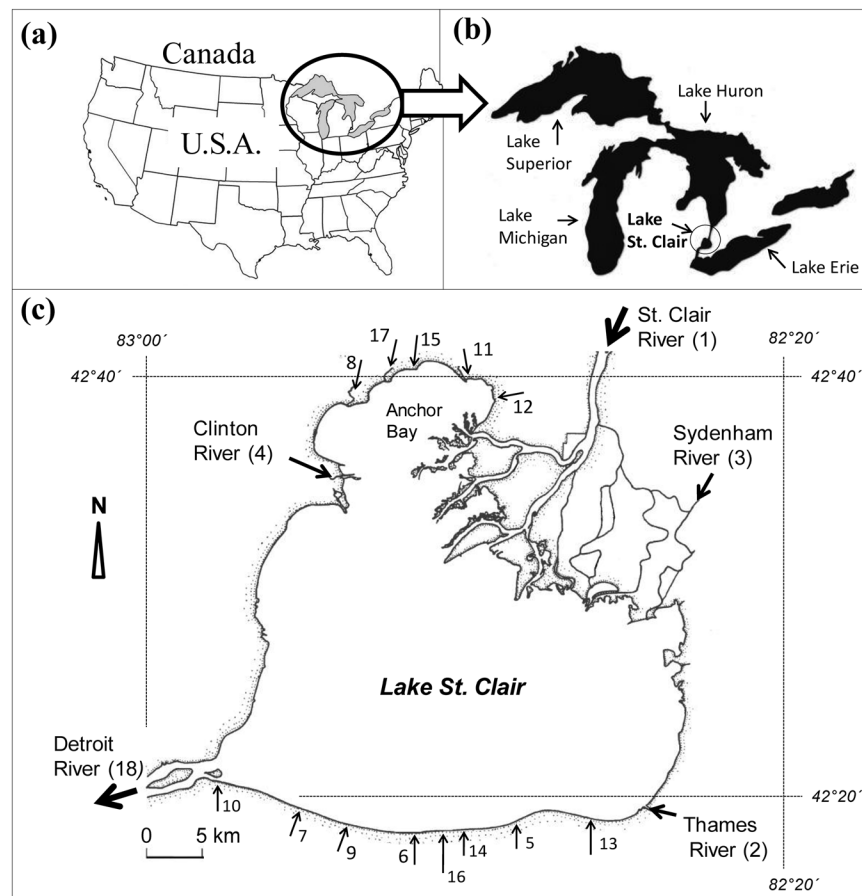


Figure 1. (a and b) Map of the Laurentian Great Lakes System; (c) map of Lake St. Clair, with arrows indicating the tributaries included in the model with their numbers corresponding to names in supporting information Tables S6, S8, and S9.

driver for CAEDYM. The latter is an ecological model capable of simulating major nutrient cycles and biota dynamics (Hipsey, 2008; Hipsey & Hamilton, 2008). ELCOM-CAEDYM has been used widely for large North American lakes, including but not limited to Lake Erie, for investigating nutrient and phytoplankton dynamics (e.g., Leon et al., 2011), effects of meteorological parameters on the lake's thermal structure (e.g., Liu et al., 2014), effects of ice cover and winter conditions on water quality (e.g., Oveisy et al., 2014), effects of nutrient loads and climatic conditions on the hypolimnetic dissolved oxygen concentrations (Bocaniov et al., 2016; Bocaniov & Scavia, 2016), effects of low dissolved oxygen conditions on the observed spatial distribution of mussels (Karatayev et al., 2018), and the effect of mussel grazing on phytoplankton biomass (Bocaniov et al., 2014a).

For this application (supporting information Figure S1 and Tables S1–S4; for table and figure numbers starting with “S” see supporting information), we simulated dynamics of phosphorus, nitrogen, and silica (e.g., phosphorus cycle; supporting information Figure S2), and five functional groups of phytoplankton as described in previous publications (Bocaniov et al., 2016; Leon et al., 2011) and supporting information Tables S3 and S4. While we do not simulate mussels and zooplankton as state variables, their grazing effect on phytoplankton is accounted for in phytoplankton loss rates.

2.3. Model Setup

We applied the model to estimate whole-lake and within-lake water retention times and whole-lake nutrient loss rates on monthly scales in Lake St. Clair, a large (1115 km², 4.25 km³) shallow polymictic lake with a mean depth of slightly less than 4 m (supporting information Table S5). Located in the connecting channel between Lakes Huron and Erie (W82°23'–W82°55' and N42°15'–N42°45'; Figures 1a and 1b), the lake processes water from the upper Great Lakes (Superior, Michigan, Huron), as well as from its proximate 15,000 km² watershed (supporting information Table S6). The watershed is approximately 60% in Canada and 40% in the United States (Baustian et al., 2014). The lake is oligotrophic in the north-western part and mesotrophic in the south-eastern part (supporting information Table S7).

The lake has many tributaries (Figure 1c; supporting information Tables S8 and S9), but the St. Clair River supplies more than 97% of the flow and a significant portion of the nutrient load (supporting information Tables S8 and S9). Three other rivers, the Thames, Sydenham, and Clinton, also contribute significant nutrient loads. While the more than 13 other tributaries are not significant sources of either nutrient load or flow, they are important for the overall water and nutrient budgets and nearshore nutrient dynamics.

Bathymetry was obtained from the National Oceanic and Atmospheric Administration (NOAA; www.ngdc.noaa.gov/mgg/greatlakes/), and we used a computational grid resolution of 500 m × 500 m in horizontal and 0.15–0.26 m in vertical dimension to represent Lake St. Clair by the 3-D Cartesian coordinates (x, y, z) in an orthogonal coordinate system. There are a total of 4,460 horizontal wet grid cells at the surface and 50 layers in the vertical, totaling 124,700 wet cells for the lake. In defining the shoreline, we used a minimum cell depth of 0.01 m. Preliminary simulations using 2 and 5 min time steps showed no noticeable differences, so a 5 min time step was used and hourly output was saved for calculating daily values and further analysis. The model was run from 15 March to 10 November inclusive for both calibration (2009) and validation (2010) years.

2.4. Boundary Conditions

The total drainage area as well as the area of land upstream from a hydrometric gauging station for each lake's tributary (supporting information Table S6) were delineated using a topographic map with 30 m × 30 m resolution grid. Tributary inflows and the Detroit River outflow were based on data from hydrometric gauging stations (supporting information Table S6) operated by either USGS (<https://waterdata.usgs.gov/nwis/>) or WSC (<https://wateroffice.ec.gc.ca/>) operated by Environment and Climate Change Canada (ECCC). Where gauge locations did not represent the entire drainage area, the ratio of the entire watershed area to the monitored area was used to scale up the daily measured flow. For very small unmonitored tributaries, precipitation amount and timing and runoff coefficients were assumed to be the same as in the nearest monitored watershed (supporting information Table S6). Flows from the St. Clair River were distributed into Lake St. Clair through its major channels (Figure 1c): North Channel (33% average flow), Middle Channel (20% flow), South Channel (18% flow), St. Clair Cutoff (20% flow), Basset Channel (4% flow), and Chenal Escarté (5%) (Bolsenga & Herdendorf, 1993).

Tributary water temperatures and water quality concentrations were gathered from a variety of data sources including the Michigan Department of Environmental Quality (MDEQ) (M. Alexander, personal communication, 22 July 2016), USGS (<http://tinyurl.com/ybfm4263>; accessed date 11 October 2016), STOrage and RETreival database (STORET) housed by the United States Environmental Protection Agency (USEPA) (<http://tinyurl.com/ydgconlz>; accessed date 26 October 2016), Provincial Water Quality Monitoring Network (PWQMN; Ontario, Canada) (<http://tinyurl.com/ycdvdj7w>; accessed date 5 December 2016), Essex Region Conservation Authority (ERCA) (K. Stammler, personal communication, 21 April 2017), other local water protection and conservation agencies (Healy et al., 2007; Nürnberg & LaZerte, 2015; RMP, 2006) and published literature (Maccoux et al., 2016). Daily water temperatures for the St. Clair River were derived from satellite-based observations of water surface temperatures in the southern part of Lake Huron in the vicinity of the outfall to the St. Clair River from the Great Lakes Surface Environmental Analysis (GLSEA) website (<http://tinyurl.com/83tarmr>; accessed date 12 December 2016). Total direct atmospheric load of nutrients to the lake surface was based on Maccoux et al. (2016).

Meteorological drivers were based on measurements at the Detroit Metropolitan Airport, corrected for differences between over-land and over-lake conditions based on empirical relationships developed by Schwab and Morton (1984), and Schertzer et al. (1987). Incoming longwave radiation was calculated first for the clear sky conditions (Idso & Jackson, 1969) and then adjusted for cloud cover (Parkinson & Washington, 1979). Over-lake precipitation was obtained from NOAA Great Lakes Environmental Research Laboratory (GLERL) website on hydrologic data for Lake St. Clair (<https://tinyurl.com/yax3eqnj>; accessed date 2 February 2017).

2.5. Initialization, Calibration, and Validation

The model was initialized with uniform lake-wide concentrations of water quality parameters, based on the first available spring observations at the lake's outflow. Water surface elevation was initialized with average water levels recorded at the St. Clair Shores, MI station (station 9034052, supporting information Figure S3d; <http://tinyurl.com/ycyhqq76>; accessed date 15 December 2016) and the Belle River, ON station (station 11965, supporting information Figure S3d; <http://tinyurl.com/ybbgdzm4>; accessed date 15 December 2016). Initial lake water temperature was based on the satellite-derived observed water surface temperatures available at the GLSEA website described above (accessed date 12 January 2017). The model was calibrated for 2009 conditions and then validated with 2010 boundary conditions (see supporting information Table S4 for calibration coefficients).

Observations for calibration and validation came from a variety of sources. Daily water level data and lake-averaged water surface temperature were based on observations at the two water level gauging stations and satellite-derived observations described above. Hourly water surface temperature was based on measurements at the in-lake buoy in the center of the lake (station 45147, supporting information Figure S3d) operated by ECCC (<http://tinyurl.com/y94ksha7>; accessed date 5 November 2016). Instantaneous measurements of water temperatures for the lake outflow were available from STORET and the Water Works Park Plant intake (the Belle Isle water intake, supporting information Figure S3a; M. Semegen, personal communication, 22 February 2017). Chemical and biological concentrations for the in-lake conditions were based on in-lake water quality monitoring stations and field surveys, as well as data from the public water intakes, from the following sources and databases: STORET (<http://tinyurl.com/ydgconlz>; accessed date 26 October 2016), STAR (Great Lakes Water Quality Database) housed by ECCC (A. Dove, personal communication, 1 February 2017), Ontario Drinking Water Surveillance Program (DWSP) operated by the Ontario's Ministry of the Environment and Climate Change (MOECC) (<http://tinyurl.com/y6vblo3>; accessed date 3 March 2017), Great Lakes Water Authority (GLWA) in Detroit (M. Semegen, personal communication, 22 February 2017; the Water Works Park water intake), and the data residing in the online database called Huron to Erie Drinking Water Monitoring Network (<http://hetestweb.azurewebsites.net/>; accessed date 23 February 2017). Satellite images (Landsat 7) from summer months in 2009 and 2010 were downloaded from Google Earth Engine (<https://earthengine.google.com/>). Data gaps caused by the satellite's Scan Line Corrector failure were filled using focal analysis in ERDAS Imagine (ERDAS: Earth Resources Data Analysis System), and images were enhanced to highlight color differences.

2.6. Lake-Wide Flushing Time and Nutrient Loss Rates

Lake-wide flushing time (FT) was calculated for each month as the ratio of the mean water volume (V , m^3) to the mean volumetric flow rate through the lake (Q , $m^3 d^{-1}$) for that month:

$$FT = \frac{V}{Q} \quad (1)$$

Lake-scale nutrient loss rates were calculated from model output by assuming the lake acts as a Continuously Stirred Tank Reactor (CSTR) with nonconservative behavior of water column nutrients represented as first-order decay. Under those conditions, the change in nutrient concentration can be represented as:

$$V \cdot \frac{dC}{dt} = W - Q \cdot C - K \cdot V \cdot C \quad (2)$$

where C is the lake-wide daily nutrient concentration (mg L^{-1}); V is the lake daily volume (m^3); W is the rate of external nutrient supply (mg d^{-1}); Q is the daily flow ($\text{m}^3 \text{d}^{-1}$); and K is the overall nutrient loss rate (d^{-1}). For dissolved phosphorus, K represents phytoplankton uptake. For total phosphorus, K represents loss to the sediments. The solution of equation (2) at time t is:

$$C = \frac{W}{Q+K \cdot V} \cdot \left(1 - e^{-\left(\frac{Q}{V} + K\right) \cdot t}\right) + C_o \cdot e^{-\left(\frac{Q}{V} + K\right) \cdot t} \quad (3)$$

where C_o , the initial average lake nutrient concentration (mg L^{-1}).

To estimate the total phosphorus (TP) and dissolved reactive phosphorus (DRP) loss rates, K_{TP} and K_{DRP} , we solved equation (3) iteratively, using values of K in increments of 0.001, until the resulting time-course of C matched the time course of lake-averaged concentrations derived daily from ELCOM-CAEDYM based primarily on the Root Mean Squared Error (RMSE).

2.7. Spatial-Dependent Water Age and Residence Time

Water age is defined here as the time it takes an individual water parcel to reach a specific location from the time it entered the model from one of its boundaries (wa_i) (Bolin & Rodhe, 1973; Deleersnijder et al., 2001; Delhez et al., 1999). We used the model to simulate the age of water at each grid cell (wa_i), a scalar tracer that is introduced to the model domain with the inflowing water from the tributaries with zero age. At the start of simulation, wa_i for each water cell was set to zero. After entering the domain, the tracer is transported as a scalar ageing with time (Hodges & Dallimore, 2014; Silva et al., 2014). We calculated spatial maps of mean monthly wa_i for the surface layer (depth: 0.2 m), the bottom layer, and a depth-integrated value. However, because the shallow lake is well mixed vertically during the entire simulation period, there were no significant differences in water age among the 3 layers, we used the surface layer in further analysis. We derived monthly lake-wide values of area-weighted and volume-weighted averages, normalized by lake area (A) and volume (V) as:

$$\overline{WA}_a = \frac{\sum_{i=1}^{i=n} (wa_i \cdot a_i)}{A} \quad (4)$$

$$\overline{WA}_v = \frac{\sum_{i=1}^{i=n} (wa_i \cdot v_i)}{V} \quad (5)$$

where \overline{WA}_a and \overline{WA}_v are area-weighted and volume-weighted average water age for the entire lake; wa_i , a_i , and v_i are the monthly mean water age (days), area (m^2), and volume (m^3) for each water cell i ; n is the overall number of water cells in either the lake area or volume; and A and V are monthly mean area (m^2) and volume (m^3) of the entire lake.

Water residence time (WRT), defined here as the time it takes water from all locations to exit the lake. To calculate WRT , we conducted a series of conservative tracer experiments with the calibrated model. Inflows, outflows, initial lake conditions, and atmospheric forcing were the same as the calibration and validation efforts; however, tributary concentrations of the tracer were set to zero. On the first day of each month between April and October in 2009 and 2010, we set the tracer concentration throughout the entire domain to 100 mg L^{-1} for 24 h. Then after those first 24 h, WRT was calculated for each month as the time it took the lake-averaged tracer concentration to drop below 5% of the initial concentration. Unlike the integrative system measure, FT , that describes water retention without accounting for the influence of spatial distribution of the underlying physical processes (Geyer et al., 2000), water age (wa_i) and WRT are measures that do account for the spatial and temporal distribution of advection and dispersion processes (Monsen et al., 2002).

3. Results

3.1. Long-Term Patterns of Discharge for the Three Major Tributaries

Discharge in 2009 was larger than in 2010 (Figure 2; supporting information Tables S8 and S9). Long-term seasonal variability in mean monthly discharge of the Thames River is much larger than that of the Clinton River (Figure 2d). The Thames had very high spring discharge and very low summer discharge relative to the annual mean. Mean monthly flows for the St. Clair River were relatively constant and the Clinton River pattern is intermediate between the Thames and St. Clair rivers (Figure 2e).

3.2. Model Calibration and Validation

The model reproduced temperatures as lake-wide averages (Figures 3a and 3c), at the lake outlet (Figures 3b and 3d), and at the location of the midlake buoy (Figures 4b and 4d) for both the calibration (2009, RMSE = 0.97°C) and validation (2010, RMSE = 1.30°C) years. Simulated water levels (Figures 4a and 4c) had an RMSE of 0.033 and 0.048 m in 2009 and 2010, respectively, representing about 0.8% and 1.3% of the mean depth in those years. Simulated water quality was also consistent with observations at the lake outlet for both the calibration (Figure 5) and validation (Figure 6) years, and the spatial distributions of surface chlorophyll matched the true color images from Landsat 7 for summer months in 2009 and 2010 (Figure 7). The model's ability to simulate temporal and spatial dynamics in nearshore water quality (supporting information Figure S3) was also quite good (supporting information Figures S4–S10) considering that the

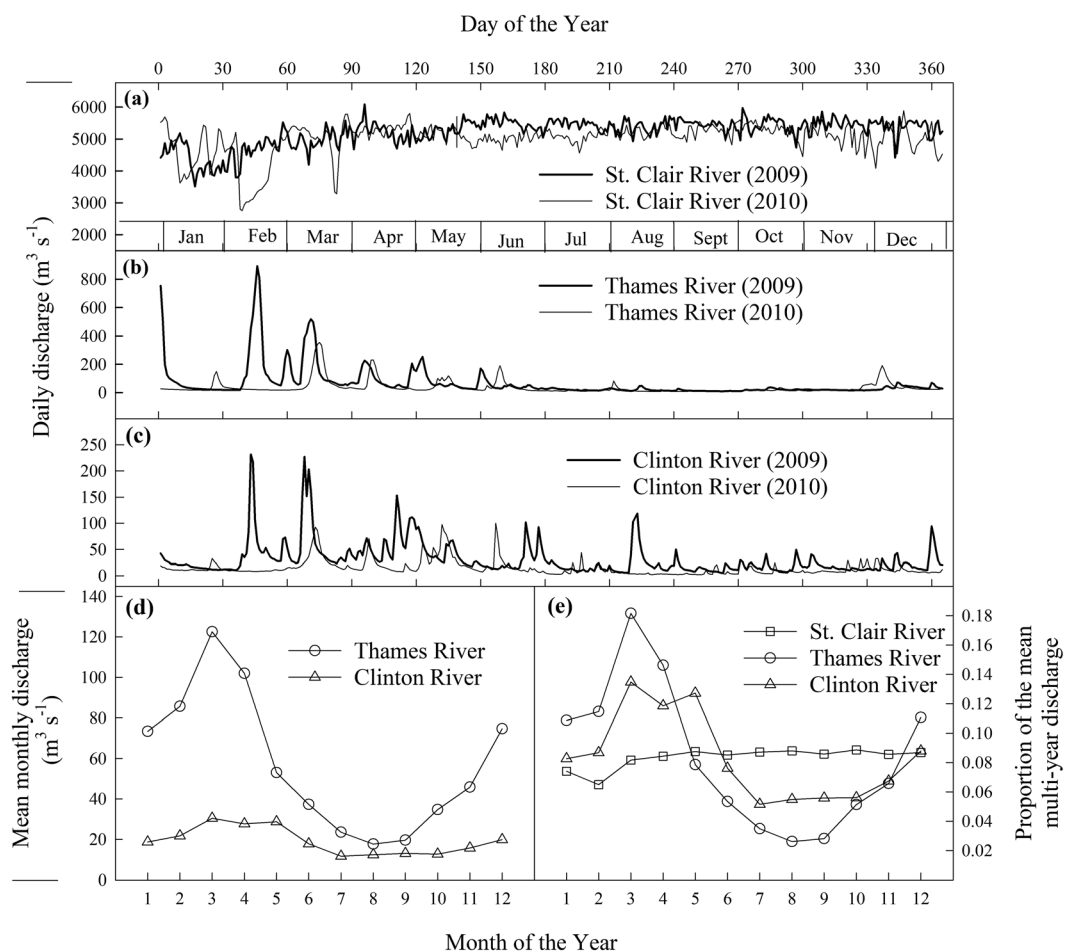


Figure 2. Daily river discharges in 2009 and 2010 for the (a) St. Clair River at Port Huron, (b) Thames River at Thamesville, and (c) Clinton River at the Moravian Drive at Mt. Clemens; (d) mean monthly discharges for the Thames and Clinton Rivers averaged over 2000 to 2016 inclusive, and (e) mean monthly discharges for the St. Clair, Thames and Clinton Rivers as a proportion of their mean annual discharge averaged over 2000–2016 for the Thames and Clinton Rivers and 2009–2016 for the St. Clair River.

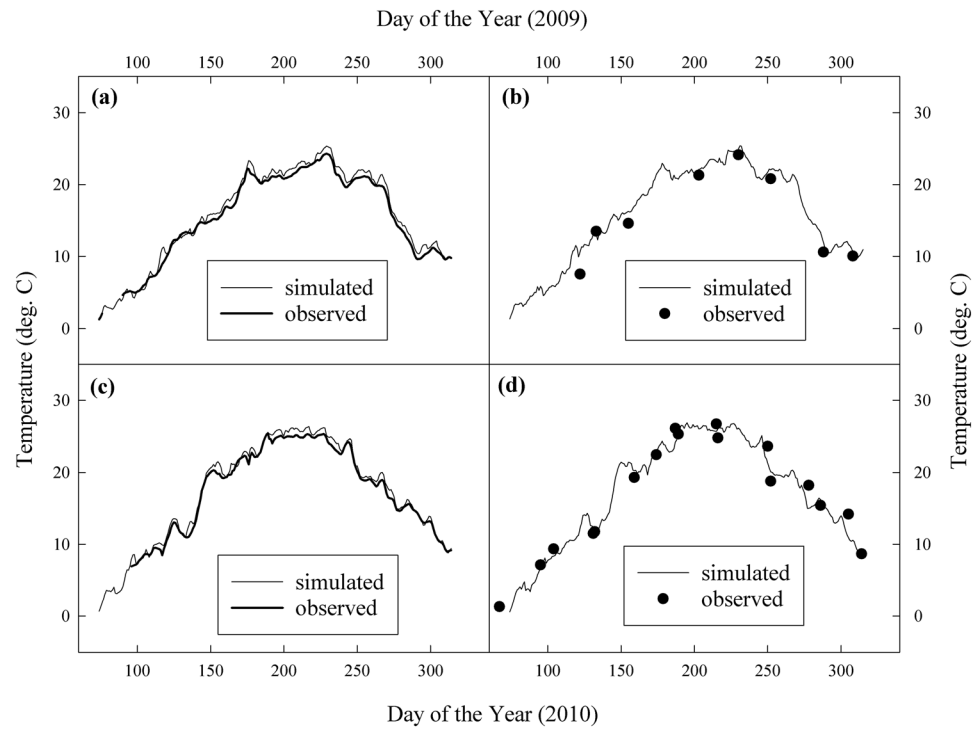


Figure 3. Comparison of modeled daily lake-wide water surface temperature with satellite-based observations for (a) 2009 and (c) 2010, and modeled and observed daily surface temperatures for the Detroit River at the lake outlet (stations 820414 and Water Works Park; supporting information Figure S3a and S3b) for (b) 2009 and (d) 2010.

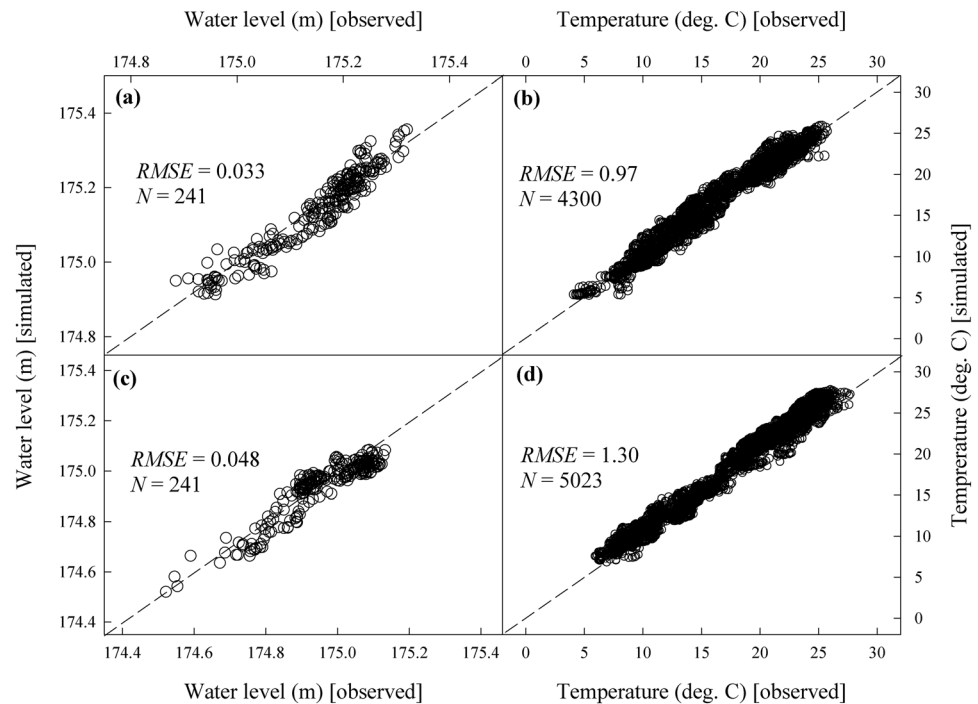


Figure 4. Comparison of modeled and observed average daily water levels for (a) 2009 and (c) 2010, and comparison of modeled hourly water surface temperature with those measured at the in-lake buoy (station 45147; supporting information Figure S3d) for (b) 2009 and (d) 2010.

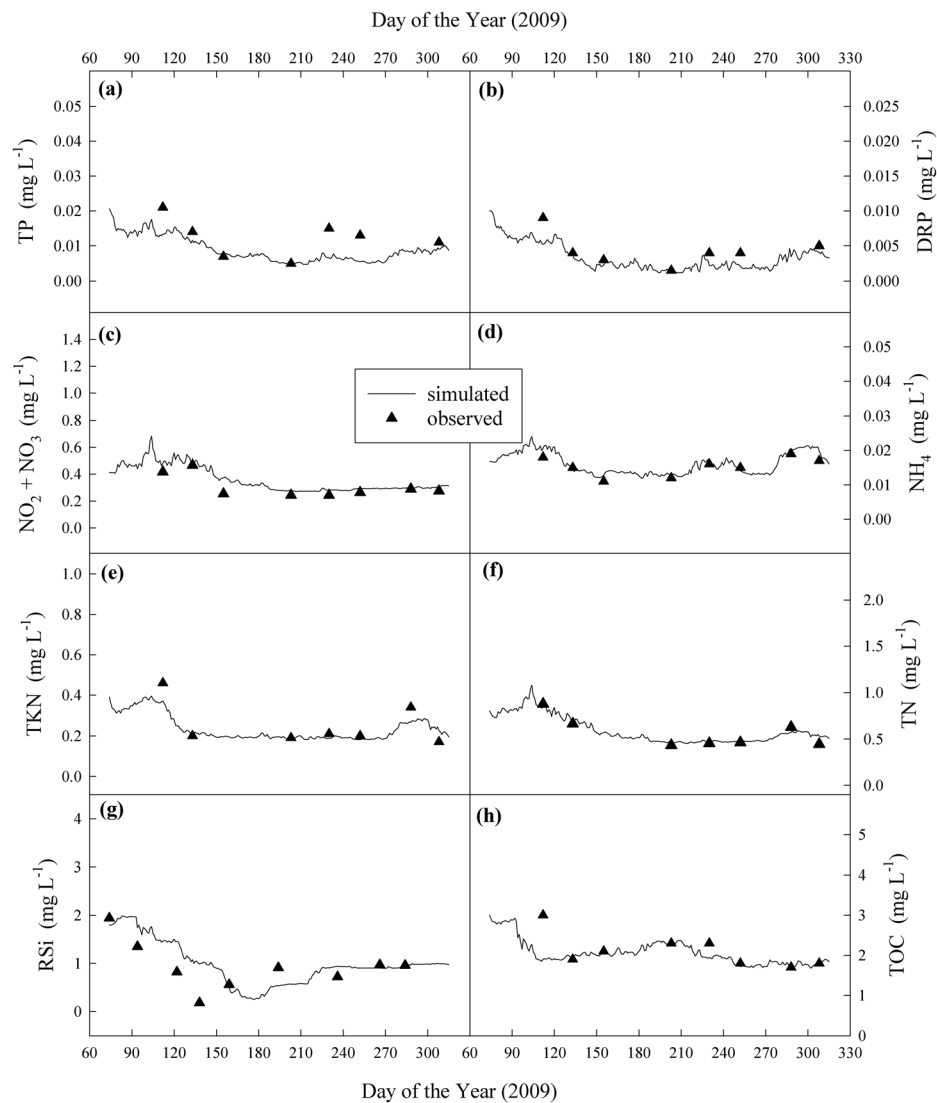


Figure 5. Modeled and observed concentrations of (a) total phosphorus (TP), (b) dissolved reactive phosphorus (DRP), (c) nitrate plus nitrite ($\text{NO}_3 + \text{NO}_2$), (d) ammonia (NH_4), (e) total Kjeldahl nitrogen (TKN), (f) total nitrogen (TN), (g) dissolved reactive silica (RSi), and (h) total organic carbon (TOC) in 2009 for the lake outlet (Detroit River, station 820414; see supporting information Figure S3b).

observations are very close to shore and at spatial resolutions much smaller than the model resolution. The RMSEs for all water quality observations at the in-lake stations were slightly elevated but all within one standard deviation of the observations (Table 1).

3.3. Validation of Hydrodynamics and Lake Circulation

Water age (w_a) is a very sensitive, time integrated measure of hydrodynamic processes that can serve as indicators of hydrodynamics for each unique location (e.g., D. Schwab, personal communication, 20 February 2017; Li et al., 2010). The spatial pattern in simulated mean monthly water age (Figures 8 and 9) was in good agreement with previous modeling results (Anderson & Schwab, 2011; Schwab et al., 1989), taking into account different boundary conditions among the studies. For example, similar to Anderson and Schwab (2011), our results indicated that the water age in the north and western lake and along the shipping channel was less than 5 days, with some areas (Anchor Bay) less than 1 day. Our results also showed older water in the eastern and southern lake (10–20 days), *albeit* with a smaller range compared to the range of 10–35 days in Anderson and Schwab (2011). The latter study modeled w_a for 1985 with only four tributaries (St. Clair, Thames, Clinton, and Sydenham rivers), with the St. Clair River and Detroit River flows

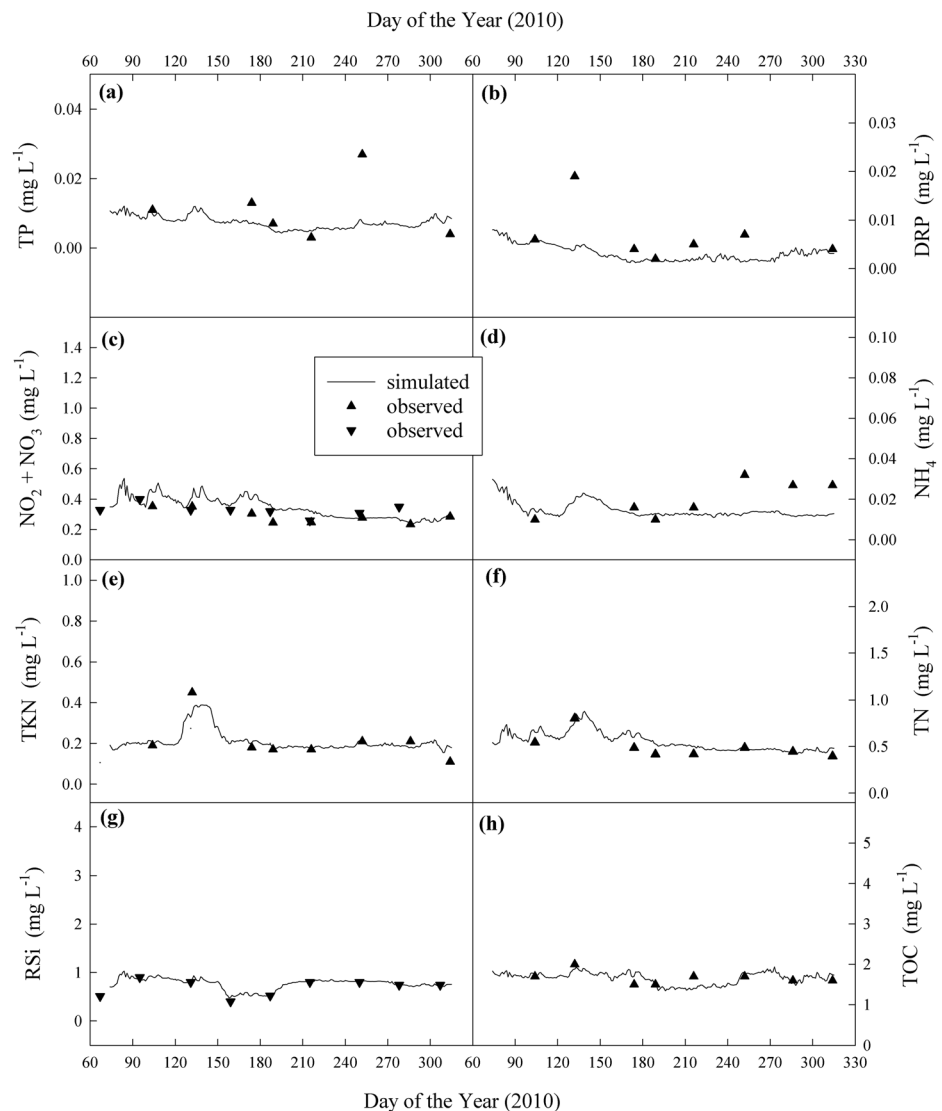


Figure 6. Modeled and observed concentrations of (a) total phosphorus (TP), (b) dissolved reactive phosphorus (DRP), (c) nitrate plus nitrite ($\text{NO}_3 + \text{NO}_2$), (d) ammonia (NH_4), (e) total Kjeldahl nitrogen (TKN), (f) total nitrogen (TN), (g) dissolved reactive silica (RSi), and (h) total organic carbon (TOC) in 2010 for the lake outlet (Detroit River, station 820414; supporting information Figure S3b).

driven by difference in water levels near Lake Huron and Lake Erie, and with flows from other tributaries treated as long-term means. In contrast, we used measured Detroit River outflow and inflows for 17 tributaries in 2009 and 2010. This included many of those directly discharging to the southern part of the lake (Figure 1c) that may have contributed to shorter residence times.

3.4. Phosphorus Loss Rates and Retention Times

Mean monthly TP loss rates (K_{TP}) ranged between 0.014 and 0.080 d^{-1} for 2009 and 2010, with maximum values in summer and minimum values in spring and fall (Table 2). Mean monthly DRP loss rates (K_{DRP}) varied more seasonally (0.01–0.24 d^{-1}) and were on average as twice the TP loss rates (Table 2), but following a similar seasonal pattern.

3.5. Flushing Time, Spatially Dependent Water Age, Mean Area-Weighted and Volume-Weighted Water Age, and Water Residence Time

Flushing time (FT) varied little (8.5–9.6 days) with maximum values in summer (Figures 10a and 10c) and a pooled 2009 and 2010 mean ($\pm\text{SD}$) of 9.1 ± 0.42 days. Water age (wa_i) exceeded FT for 40–60% of the lake

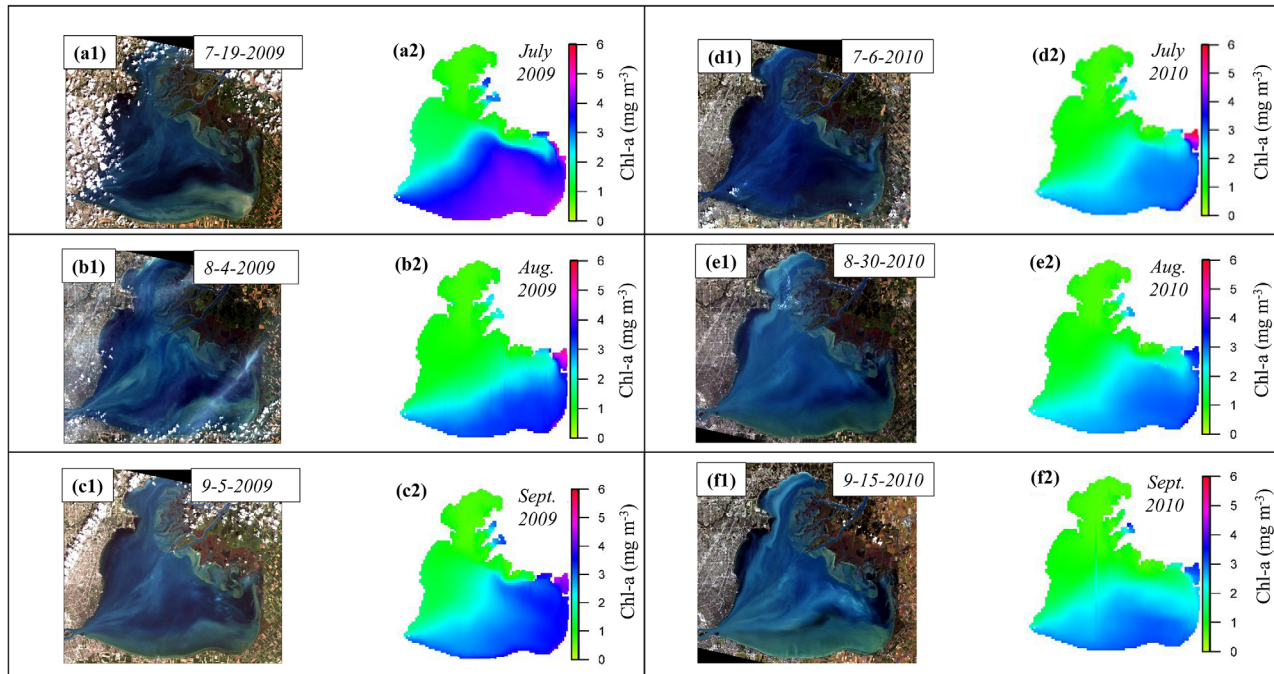


Figure 7. Comparison of true color Landsat 7 satellite images (a1–f1) with simulated Chlorophyll-a (Chl-a; mg m^{-3}) distributions (a2–f2) for summer 2009 and 2010.

area during April–November (Figures 10b and 10d). While the pooled means for area-weighted \overline{WA}_a and volume-weighted \overline{WA}_v were similar to the FT of 9 days (8.5 ± 1.4 days and 8.9 ± 1.4 days, respectively), there was substantial seasonal variability, with \overline{WA}_a ranging from 6.1 to 10.3 days and \overline{WA}_v from 6.4 to 10.9 days (Figures 10a and 10c). Water residence time (WRT) was approximately 3 times longer than FT , \overline{WA}_a , and \overline{WA}_v , with an overall pooled mean of 28 ± 4 days. It was shorter in spring (24.5 ± 2.4 days; $N = 4$) and fall (26.0 ± 2.6 days; $N = 4$), and longer in summer (June–August; 31.0 ± 2.3 days; $N = 6$).

Water age had substantial temporal and spatial variability, and there were two clearly distinct regions (Figures 8 and 9); one with values of $wa_i < 5$ days in the north-western region and one with higher values (>7 days) in the south-eastern part. While the north-western region varied little over time, the south-eastern region was very dynamic seasonally, with mean monthly values increasing from 7 days in March to about 20 days in June–August, and then decreasing into November. The delineation of these two regions is consistent with previous segmentations based on the observed water quality and zooplankton densities (David et al., 2009).

Table 1
Comparison of Modeled and Measured in-Lake Water Quality Properties

Parameter	Year	N	Mean		SD_o	RMSE	RSR
			Field observations	Predictions			
TP	2009	57	0.0194	0.0176	0.0197	0.0139	0.70
$\text{NO}_3 + \text{NO}_2$	2009	55	0.3844	0.3958	0.4509	0.0355	0.19
NH_4	2009	13	0.0171	0.0161	0.0052	0.0038	0.73
TOC	2009	45	2.4044	2.1045	0.7568	0.6098	0.81
Chl-a	2009	222	0.0009	0.0011	0.0008	0.0009	1.13
TP	2010	60	0.0142	0.0128	0.0099	0.0051	0.52
$\text{NO}_3 + \text{NO}_2$	2010	71	0.4047	0.4260	0.5368	0.0220	0.04
NH_4	2010	64	0.0308	0.0231	0.0231	0.0131	0.57
TOC	2010	26	2.5385	2.0962	0.9304	0.7413	0.80
Chl-a	2010	191	0.0015	0.0012	0.0011	0.0011	1.04

Note. All units are mg L^{-1} . The following abbreviations were used: N , number of compared pairs; SD_o , standard deviation of observations; $RMSE$, root mean squared error; RSR , $RMSE$ -observation standard deviation ratio defined as a ratio of $RMSE$ to the standard deviation of the observations.

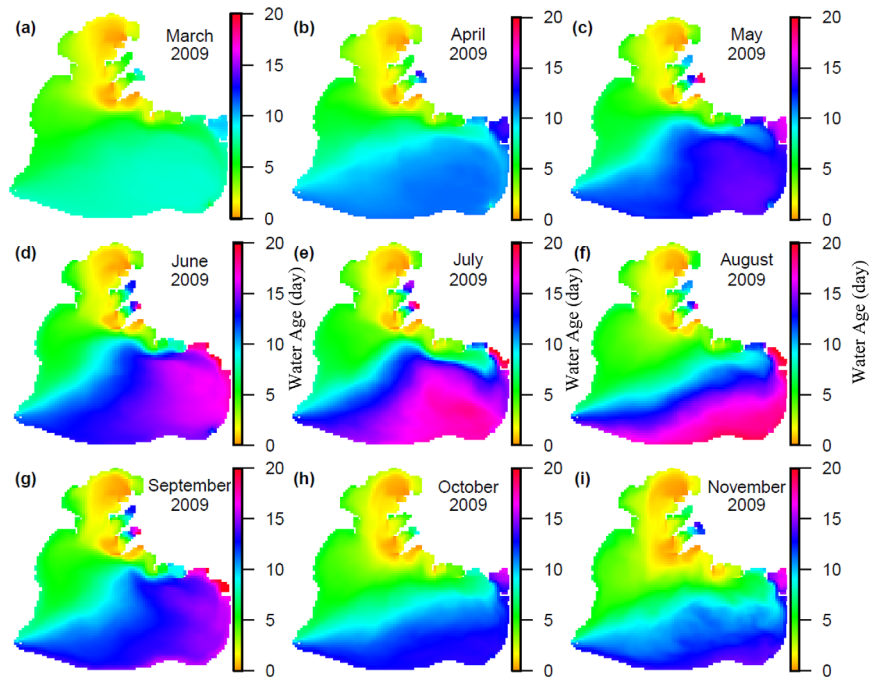


Figure 8. Simulated mean water age (wa_i ; in days) for each month in 2009 at the depth of 0.2 m. Results for the bottom layer and a depth-integrated layer are essentially the same.

3.6. Nutrient Loss Rates and Phytoplankton Dynamics

To explore the relationship between nutrient loss rates and measures of FT , WRT , \overline{WA}_a , and \overline{WA}_v (supporting information Figure S11), we performed ordinary least squares linear regressions on the monthly data with loss rate as the dependent variable (Table 3). Although all regressions were significant, \overline{WA}_a and \overline{WA}_v had the strongest explanatory power based on R^2 , P value, and F ratio. Areas of elevated phytoplankton biomass

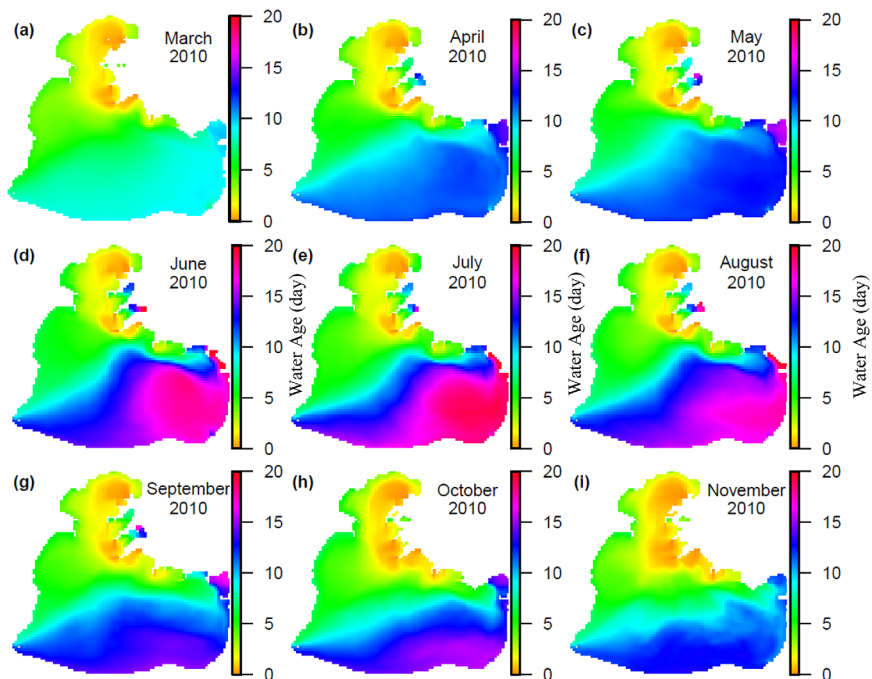


Figure 9. Simulated mean water age (wa_i ; in days) for each month in 2010 at the depth of 0.2 m. Results for the bottom layer and a depth-integrated layer are essentially the same.

Table 2
Calculated Monthly Mean (\pm SD) Lake-Wide Nutrient Loss Rates (K_{TP} and K_{DRP} ; d^{-1}) for Total and Dissolved Reactive Phosphorus (TP and DRP, Respectively)

#	Month	K_{TP}		K_{DRP}	
		(d^{-1})	(d^{-1})	(d^{-1})	(d^{-1})
		2009	2010	2009	2010
1	Mar	0.018	0.014	0.010	0.008
2	Apr	0.025	0.020	0.020	0.010
3	May	0.025	0.045	0.025	0.050
4	Jun	0.070	0.060	0.200	0.200
5	Jul	0.075	0.080	0.240	0.190
6	Aug	0.075	0.075	0.150	0.160
7	Sept	0.080	0.045	0.200	0.170
8	Oct	0.025	0.030	0.055	0.075
9	Nov	0.025	0.022	0.035	0.045
Average:		0.046 ± 0.027	0.043 ± 0.024	0.104 ± 0.092	0.101 ± 0.079

(Figures 7, 11, and 12), with largest biomass in June (Figures 11d and 12d), are consistent with the temporal and spatial dynamics of the south-eastern zone's "older" water. Our spatial patterns and seasonal dynamics of phytoplankton (Figures 7, 11, and 12), as well as higher DRP loss rates in summer (e.g., K_{DRP} ; Table 2), are consistent with previous results (e.g., Munawar et al., 1991) that report phytoplankton biomass peaking in June and its specific photosynthetic activity (typically associated with assimilation of dissolved nutrients) highest in summer.

4. Discussion

There have been other efforts to estimate water residence times in the Great Lakes. Anderson and Schwab (2011) estimated transport time scales for Lake St. Clair with a three-dimensional hydrodynamic model that

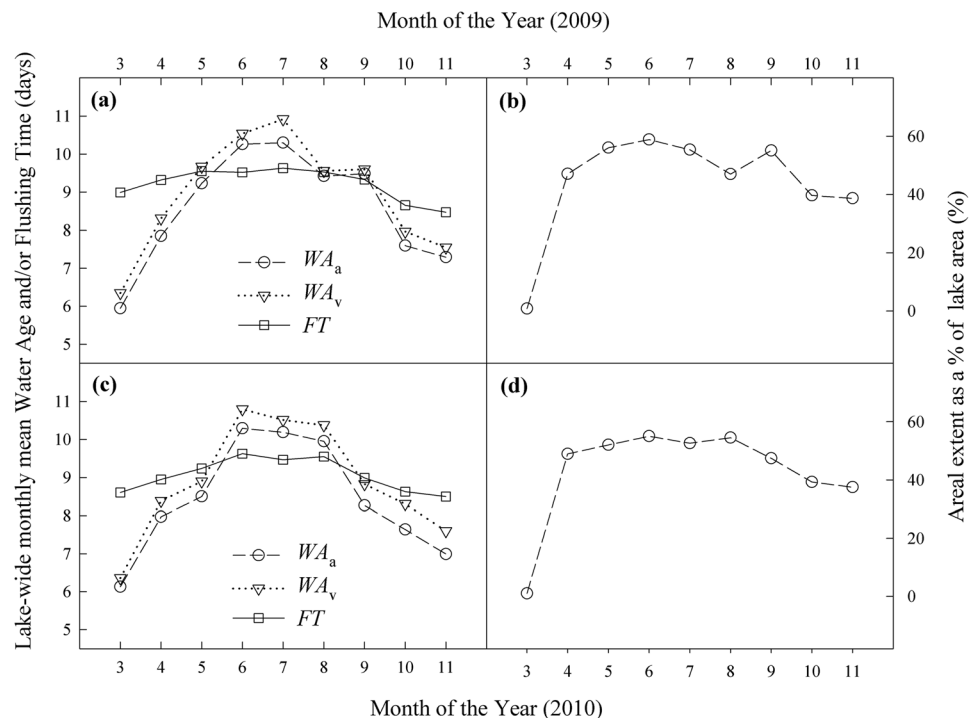


Figure 10. Area-weighted (\overline{WA}_a) and volume-weighted (\overline{WA}_v) averages of lake-wide water age and flushing time (FT) for each month in (a) 2009 and (c) 2010; temporal development of the areas with \overline{WA}_a exceeding the lake's average flushing rate (9 days) expressed as the percentage of the entire lake area in (b) 2009 and (d) 2010.

Table 3

Linear Least Squares Regressions relating monthly Nutrient Loss Rates for Total and Dissolved Reactive Phosphorus (K_{TP} and K_{DRP}) to Various Scales of Water Exchange: Flushing Time (FT), Area-Weighted (\overline{WA}_a) and Volume-Weighted (\overline{WA}_v) Lake-Wide Averages of Water Age, and Lake-Wide Water Retention Time (WRT)

Model	Dependent variable	Regression	R^2	P value	N	F ratio
1	K_{TP}	$-0.357(\pm 0.092) + 0.044(\pm 0.010)[FT]$	0.547	0.000	18	19.30
2	K_{TP}	$-0.084(\pm 0.018) + 0.015(\pm 0.002)[\overline{WA}_a]$	0.760	0.000	18	50.76
3	K_{TP}	$-0.087(\pm 0.021) + 0.015(\pm 0.002)[\overline{WA}_v]$	0.715	0.000	18	40.09
4	K_{TP}	$-0.085(\pm 0.032) + 0.005(\pm 0.001)[WRT]$	0.602	0.001	14	18.14
5	K_{DRP}	$-1.049(\pm 0.348) + 0.126(\pm 0.038)[FT]$	0.407	0.004	18	11.00
6	K_{DRP}	$-0.305(\pm 0.069) + 0.048(\pm 0.008)[\overline{WA}_a]$	0.692	0.000	18	36.00
7	K_{DRP}	$-0.327(\pm 0.073) + 0.048(\pm 0.008)[\overline{WA}_v]$	0.688	0.000	18	35.23
8	K_{DRP}	$-0.338(\pm 0.112) + 0.017(\pm 0.004)[WRT]$	0.589	0.001	14	17.23

Note. See sections 2.6 and 2.7 for definitions of FR , \overline{WA}_a , \overline{WA}_v , and WRT . The following abbreviations were used: \pm , standard errors of the regression coefficients; R^2 , coefficient of determination; N , number of compared pairs; F ratio, the F ratio calculated as the Model Mean Square to the Error Mean Square.

accounts for the hydraulic effects of the St. Clair and Detroit rivers. Similar to our findings, they found the eastern and southern regions of the lake to have longer water ages (10–35 days) than the western region and along the shipping channel (5 days). Similarly, Schwab et al. (1989) reported residence times ranging from 7 to 30 days for individual lake tributaries depending on wind conditions, with an average lake residence time of 9 days based on the average depth and inflow. Oveisy et al. (2015) used six methods to estimate flushing from the Bay of Quinte (Lake Ontario), with three methods (tracer release, drifter paths, bulk residence time) converging on an estimate that the bay overall flushes 5 times a year, with isolated embayments having water ages (4–5 months) that may trap nutrients and allow sufficient time and conditions for algae blooms to occur. Katsev (2017) used overall hydraulic residence times for the individual Great Lakes to illustrate how the time scale of lake responds to external inputs of limiting nutrients can be evaluated

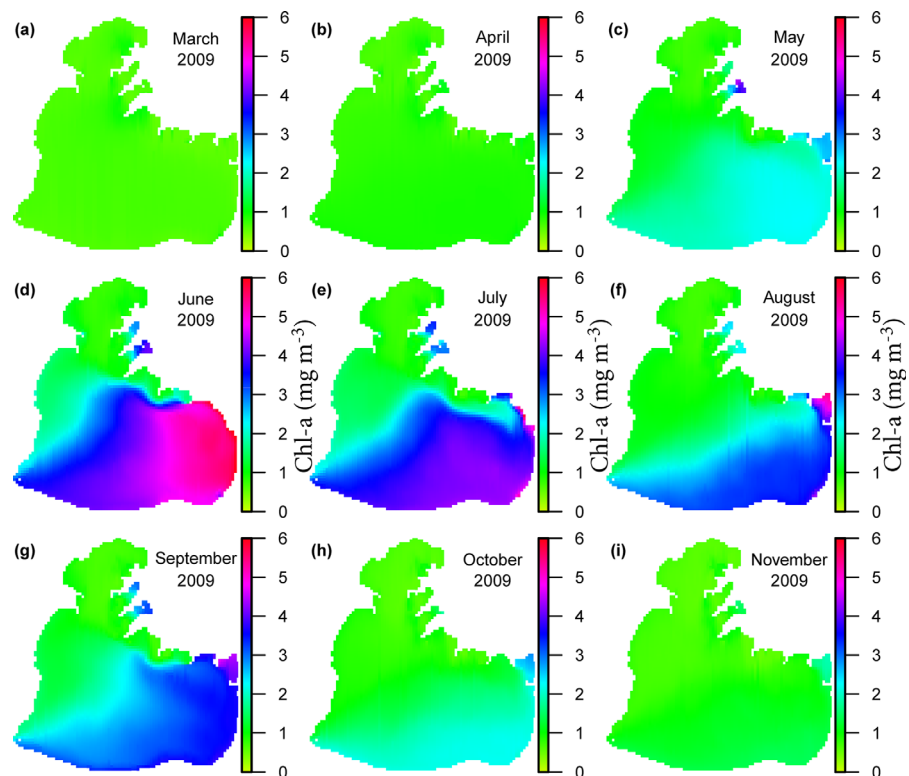


Figure 11. Simulated mean Chlorophyll-a (Chl-a; mg m^{-3}) for each month in 2009 at the depth of 0.2 m.

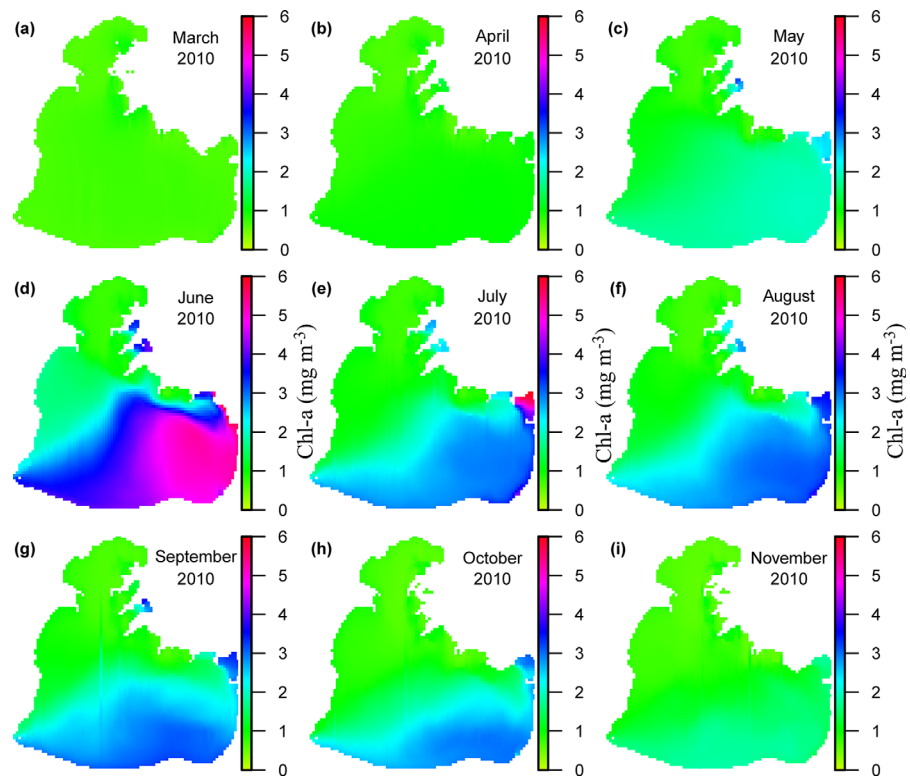


Figure 12. Simulated mean Chlorophyll-a (Chl-a; mg m^{-3}) for each month in 2010 at the depth of 0.2 m.

from a simple mass balance model that takes into account nutrient recycling in sediments. He used residence times ranging from 172 years for Lake Superior to 2.6 years for Lake Erie. Quinn (1992) used water balances to estimate residence times of 2.7 years for Lake Erie, 173 years for Lake Superior, and 0.04 years (14.2 days) for Lake St. Clair based on water balances. Quinn's larger estimate for Lake St. Clair was based on a larger lake volume (6.6 km^3 versus 4.25 km^3).

While there have been other numerical modeling studies of Lake St. Clair, including both 2-D (e.g., Holtschlag & Koschik, 2002; Schwab et al., 1989) and 3-D models (Anderson et al., 2010; Anderson & Schwab, 2011; Ibrahim & McCorquodale, 1985), with the exception of one study (Lang & Fontaine, 1990) that explored the transport of organic pollutants, this is the first time a process-based ecological model has been applied to this lake. Overall, the model accurately simulated water temperatures (Figures 3, 4b, and 4d), water levels (Figures 4a and 4c), and water quality (Figures 5–7, supporting information Figures S4–S10, and Table 1), with statistical measures of fit (e.g., RMSE, RSR; Table 1) similar to those reported in other 3-D modeling studies (e.g., Bocaniov et al., 2014b; Karatayev et al., 2018; Liu et al., 2014; Oveisy et al., 2014).

Our calculated mean flushing time (FT) was similar to that reported in earlier studies of Lake St. Clair (e.g., Bricker et al., 1976: 9.17 days; Schwab et al., 1989: 9 days). By comparing FT , average water age (\overline{WA}_a , \overline{WA}_v), and water residence time (WRT), we demonstrated that FT , which does not account for spatial variability in water movements, masks the impact of that variability. This is particularly important for this large, wind-driven shallow lake with multiple tributary inputs, and where nutrient loads and associated-ecosystem responses (e.g., water column productivity, benthic recycling of nutrients, etc.) occur on small time scales (Boynton et al., 1995; Sterner et al., 2017).

Our simulated spatial distribution of water age is also consistent with previous modeling studies (Anderson & Schwab, 2011; Schwab et al., 1989), as well as with the observed spatial distribution of specific conductance (Bricker et al., 1976), and observed and modeled spatial distribution of a conservative tracer (Lang & Fontaine, 1990). Our results illustrating the formation of two distinct zones of water age and productivity (Figures 8 and 9; 11 and 12) are in good agreement with earlier studies (e.g., David et al., 2009; Leach, 1980) that describe the general spatial and temporal distribution of two discrete water masses with less

productive north-western water dominated by the St. Clair River and more productive south-eastern water influenced by Thames, Sydenham, and other minor tributaries from Ontario.

There are large areas in the southern part of the lake with “older” water (15–20 days) during summer, suggesting longer retention times. These longer residence times support prolonged phytoplankton production and higher biomass (Figures 11 and 12; supporting information Table S7) consistent with observations (Figure 7) and previous studies (Bricker et al., 1976; David et al., 2009; Leach, 1972, 1973; Munawar et al., 1991). The elevated phytoplankton biomass and increased retention time influence DRP via phytoplankton assimilation and TP via sedimentation. The fact that wa_i is shorter in spring and fall and longer in summer—and longer in the southern part of the lake (Figures 8 and 9)—helps explain formation of the summer algal blooms in the southern part of the lake that are often observed from the remote sensing (e.g., Figure 7; supporting information Figure S12). This is also consistent with the lake-scale relationships between nutrient loss rates (K_{TP} and K_{DRP}) and area-weighted and volume-weighted water ages (\overline{WA}_a and \overline{WA}_v) (Table 3).

These distributions in time and space also have implications for P export to Lake Erie via the Detroit River, one of the key drivers of its eutrophication symptoms. For example, the nutrient load from the Thames River, which is higher in spring and fall (Figures 2d and 2e) when wa_i and WRT are shorter (e.g., Figure 10) and lake-scale nutrient loss rates are smaller (K_{TP} and K_{DRP} ; Table 2), are likely to have relatively higher export to Lake Erie. Conversely, the load from the Clinton River (Figures 2d and 2e), which typically is higher in summer when wa_i and WRT are longer (e.g., Figure 10), and nutrient losses are higher, may export relatively less to Lake Erie because of the higher losses during the summer. By combining this tributary-by-tributary relative export information with their respective loads, it should be possible to help select areas of emphasis for watershed nutrient abatement measures.

Acknowledgments

We would like to thank the following people: David Schwab and three anonymous reviewers for helpful comments and discussion, Awoke Teshager for help in delineating the drainage areas for each lake’s tributary and gauging stations, Yu-Chen Wang for help in visualizing the field data, Lynn Vaccaro for help in gathering field data, and Colleen Long for help in analyzing Landsat 7 imagery. This work was funded in part by the Fred A and Barbara M Erb Family Foundation (grant 903) and the University of Michigan Graham Sustainability Institute. The data used are listed in the references, figures, tables, supporting information, and can be available upon request by contacting the corresponding author (S. Bocaniov, sbocaniov@uwaterloo.ca).

References

- Anderson, E. J., & Schwab, D. J. (2011). Relationships between wind-driven and hydraulic flow in Lake St. Clair and the St. Clair River Delta. *Journal of Great Lakes Research*, 37, 147–158.
- Anderson, E. J., Schwab, D. J., & Lang, G. A. (2010). Real-time hydraulic and hydrodynamic model of the St. Clair River, Lake St. Clair, Detroit River system. *Journal of Hydraulic Engineering*, 136(8), 507–518.
- Baustian, M. M., Mavrommati, G., Dreelin, E. A., Esselman, P., Schultze, S. R., Qian, L., et al. (2014). A one hundred year review of the socio-economic and ecological systems of Lake St. Clair, North America. *Journal of Great Lakes Research*, 40, 15–26.
- Bertani, I., Obenour, D. R., Steger, C. E., Stow, C. A., Gronewold, A. D., & Scavia, D. (2016). Probabilistically assessing the role of nutrient loading in harmful algal bloom formation in western Lake Erie. *Journal of Great Lakes Research*, 42, 1184–1192.
- Bocaniov, S. A., Leon, L. F., Rao, Y. R., Schwab, D. J., & Scavia, D. (2016). Simulating the effect of nutrient reduction on hypoxia in a large lake (Lake Erie, USA-Canada) with a three-dimensional lake model. *Journal of Great Lakes Research*, 42(6), 1228–1240.
- Bocaniov, S. A., & Scavia, D. (2016). Temporal and spatial dynamics of large lake hypoxia: Integrating statistical and three-dimensional dynamic models to enhance lake management criteria. *Water Resources Research*, 52, 4247–4263. <https://doi.org/10.1002/2015WR018170>
- Bocaniov, S. A., Smith, R. E., Spillman, C. M., Hipsey, M. R., & Leon, L. F. (2014a). The nearshore shunt and the decline of the phytoplankton spring bloom in the Laurentian Great Lakes: Insights from a three-dimensional lake model. *Hydrobiologia*, 731(1), 151–172.
- Bocaniov, S. A., Ullmann, C., Rinke, K., Lamb, K. G., & Boehrer, B. (2014b). Internal waves and mixing in a stratified reservoir: Insights from three-dimensional modeling. *Limnologia*, 49, 52–67.
- Bolin, B., & Rodhe, H. (1973). A note on the concepts of age distribution and transit time in natural reservoirs. *Tellus*, 25(1), 58–62.
- Bolsenga, S., & Herdendorf, C. (Eds.) (1993). *Lake Erie and Lake St. Clair handbook*. Detroit, MI: Wayne State University Press.
- Boynton, W. R., Garber, J. H., Summers, R., & Kemp, W. M. (1995). Inputs, transformations, and transport of nitrogen and phosphorus in Chesapeake Bay and selected tributaries. *Estuaries and Coasts*, 18(1), 285–314.
- Brett, M. T., & Benjamin, M. M. (2008). A review and reassessment of lake phosphorus retention and the nutrient loading concept. *Freshwater Biology*, 53(1), 194–211.
- Bricker, K. S., Bricker, F. J., & Gannon, J. E. (1976). Distribution and abundance of zooplankton in the US waters of Lake St. Clair, 1973. *Journal of Great Lakes Research*, 2(2), 256–271.
- David, K. A., Davis, B. M., & Hunter, R. D. (2009). Lake St. Clair zooplankton: Evidence for post-Dreissena changes. *Journal of Freshwater Ecology*, 24(2), 199–209.
- Deleersnijder, E., Campin, J. M., & Delhez, E. J. (2001). The concept of age in marine modeling. I: Theory and preliminary model results. *Journal of Marine Systems*, 28, 229–267.
- Delhez, E. J., Campin, J. M., Hirst, A. C., & Deleersnijder, E. (1999). Toward a general theory of the age in ocean modelling. *Ocean Modelling*, 1(1), 17–27.
- Dillon, P. J., & Molot, L. A. (1996). Long-term phosphorus budgets and an examination of a steady-state mass balance model for central Ontario lakes. *Water Research*, 30(10), 2273–2280.
- Geyer, W. R., Morris, J. T., Prah, F. G., & Jay, D. A. (2000). Interaction between physical processes and ecosystem structure: A comparative approach. In J. E. Hobbie (Ed.), *Estuarine science: A synthetic approach to research and practice* (pp. 177–206). Washington, DC: Island Press.
- Healy, D. F., Chambers, D. B., Rachol, C. M., & Jodoin, R. S. (2007). *Water quality of the St. Clair River, Lake St. Clair, and their US tributaries, 1946–2005* (U.S. Geol. Surv. Sci. Invest. Rep. 2007–5172). Reston, VA: U.S. Geological Survey.
- Hipsey, M. R. (2008). *The CWR computational aquatic ecosystem dynamics model CAEDYM. User manual*. Perth, WA: Centre for Water Research, University of Western Australia.

- Hipsey, M. R., & Hamilton, D. P. (2008). *Computational aquatic ecosystem dynamics model: CAEDYM v3. v3.3 Science manual (DRAFT)*. Perth, WA: Centre for Water Research, University of Western Australia.
- Hodges, B., & Dallimore, C. (2014). *Estuary, lake and coastal ocean model: ELCOM v3.0 user manual*. Perth, WA: Centre for Water Research, University of Western Australia.
- Hodges, B., Imberger, J., Saggio, A., & Winters, K. (2000). Modeling basin-scale internal waves in a stratified lake. *Limnology and Oceanography*, *45*, 1603–1620.
- Holtschlag, D. J., & Koschik, J. A. (2002). *Two-dimensional hydrodynamic model of the St. Clair-Detroit River Waterway in the Great Lakes basin*. Reston, VA: U.S. Department of the Interior, U.S. Geological Survey.
- Ibrahim, K. A., & McCorquodale, J. A. (1985). Finite element circulation model for Lake St. Clair. *Journal of Great Lakes Research*, *11*, 208–222.
- Idso, S. B., & Jackson, R. D. (1969). Thermal radiation from the atmosphere. *Journal of Geophysical Research*, *74*, 5397–5403.
- Karatayev, A. Y., Burlakova, L. E., Mehler, K., Bocaniov, S. A., Collingsworth, P. D., Warren, G., et al. (2018). Biomonitoring using invasive species in a large lake: Dreissena distribution maps hypoxic zones. *Journal of Great Lakes Research*. <https://doi.org/10.1016/j.jglr.2017.08.001>
- Katsev, S. (2017). When large lakes respond fast: A parsimonious model for phosphorus dynamics. *Journal of Great Lakes Research*, *43*, 199–204.
- Lang, G. A., & Fontaine, T. D. (1990). Modeling the fate and transport of organic contaminants in Lake St. Clair. *Journal of Great Lakes Research*, *16*(2), 216–232.
- Leach, J. H. (1972). Distribution of chlorophyll and related variables in Ontario waters of Lake St. Clair. In Proceedings of the 15th Conference on Great Lakes Research (pp. 80–86). Ann Arbor, MI: International Association for Great Lakes Research.
- Leach, J. H. (1973). Seasonal distribution, composition and abundance of zooplankton in Ontario waters of Lake St. Clair. In Proceedings of the 16th Conference on Great Lakes Research (pp. 80–86). Ann Arbor, MI: International Association for Great Lakes Research.
- Leach, J. H. (1980). Limnological sampling intensity in Lake St. Clair in relation to distribution of water masses. *Journal of Great Lakes Research*, *6*(2), 141–145.
- Leon, L. F., Smith, R. E., Hipsey, M. R., Bocaniov, S. A., Higgins, S. N., Hecky, R. E., et al. (2011). Application of a 3D hydrodynamic-biological model for seasonal and spatial dynamics of water quality and phytoplankton in Lake Erie. *Journal of Great Lakes Research*, *37*(1), 41–53.
- Li, Y., Acharya, K., Chen, D., & Stone, M. (2010). Modeling water ages and thermal structure of Lake Mead under changing water levels. *Lake and Reservoir Management*, *26*(4), 258–272.
- Liu, W., Bocaniov, S. A., Lamb, K. G., & Smith, R. E. (2014). Three dimensional modeling of the effects of changes in meteorological forcing on the thermal structure of Lake Erie. *Journal of Great Lakes Research*, *40*(4), 827–840.
- Maccoux, M. J., Dove, A., Backus, S. M., & Dolan, D. M. (2016). Total and soluble reactive phosphorus loadings to Lake Erie: A detailed accounting by year, basin, country, and tributary. *Journal of Great Lakes Research*, *42*, 1151–1165.
- Monsen, N. E., Cloern, J. E., Lucas, L. V., & Monismith, S. G. (2002). A comment on the use of flushing time, residence time, and age as transport time scales. *Limnology and Oceanography*, *47*(5), 1545–1553.
- Munawar, M., Munawar, I. F., & Sprules, W. G. (1991). The plankton ecology of Lake St. Clair, 1984. *Hydrobiologia*, *219*(1), 203–227.
- Nixon, S. W., Ammerman, J. W., Atkinson, L. P., Berounsky, V. M., Billen, G., Boicourt, W. C., et al. (1996). The fate of nitrogen and phosphorus at the land-sea margin of the North Atlantic Ocean. *Biogeochemistry*, *35*(1), 141–180.
- Nürnberg, G., & LaZerte, B. (2015). *Water quality assessment in the Thames River watershed—Nutrient and sediment sources* (report). Baysville, ON: The Upper Thames River Conservation Authority. Retrieved from <https://tinyurl.com/ycvmohod>; assessed date 15 November 2016.
- Obenour, D. R., Gronewold, A. D., Stow, C. A., & Scavia, D. (2014). Using a Bayesian hierarchical model with a gamma error distribution to improve Lake Erie cyanobacteria bloom forecasts. *Water Resources Research*, *50*, 7847–7860. <https://doi.org/10.1002/2014WR015616>
- Oveisy, A., Boegman, L., & Rao, Y. R. (2015). A model of the three-dimensional hydrodynamics, transport and flushing in the Bay of Quinte. *Journal of Great Lakes Research*, *41*, 536–548.
- Oveisy, A., Rao, Y. R., Leon, L. F., & Bocaniov, S. A. (2014). Three-dimensional winter modeling and the effects of ice cover on hydrodynamics, thermal structure and water quality in Lake Erie. *Journal of Great Lakes Research*, *40*, 19–28.
- Parkinson, C. L., & Washington, W. M. (1979). A large-scale numerical model of sea ice. *Journal of Geophysical Research*, *84*, 311–337.
- Quinn, F. H. (1992). Hydraulic residence times for the Laurentian Great Lakes. *Journal of Great Lakes Research*, *18*, 22–28.
- RMP (2006). *Lake St. Clair Regional Monitoring Project. Water quality sampling and analysis* (final report). Mount Clemens, MI: Macomb County Health Department (October 30, 2006). Retrieved from <https://tinyurl.com/yazz9qhd>; assessed date 15 November 2016.
- Rucinski, D., DePinto, J., Beletsky, D., & Scavia, D. (2016). Modeling hypoxia in the Central Basin of Lake Erie under potential phosphorus load reduction scenarios. *Journal of Great Lakes Research*, *42*, 1206–1211.
- Scavia, D., Allan, J. D., Arend, K. K., Bartell, S., Beletsky, D., Bosch, N. S., et al. (2014). Assessing and addressing the re-eutrophication of Lake Erie: Central basin hypoxia. *Journal of Great Lakes Research*, *40*, 226–246.
- Scavia, D., DePinto, J. V., & Bertani, I. (2016). A Multi-model approach to evaluating target phosphorus loads for Lake Erie. *Journal of Great Lakes Research*, *42*, 1139–1150.
- Scavia, D., & Liu, Y. (2009). Exploring estuarine nutrient susceptibility. *Environmental Science and Technology*, *43*, 3474–3479.
- Schertzer, W. M., Saylor, J. H., Boyce, F. M., Robertson, D. G., & Rosa, F. (1987). Seasonal thermal cycle of Lake Erie. *Journal of Great Lakes Research*, *13*(4), 468–486.
- Schindler, D. W., Kling, H., Schmidt, R. V., Prokopowich, J., Frost, V. E., Reid, R. A., et al. (1973). Eutrophication of Lake 227 by addition of phosphate and nitrate: The second, third, and fourth years of enrichment, 1970, 1971, and 1972. *Journal of the Fisheries Research Board of Canada*, *30*(10), 1415–1440.
- Schwab, D. J., Clites, A. H., Murthy, C. R., Sandall, J. E., Meadows, L. A., & Meadows, G. A. (1989). The effect of wind on transport and circulation in Lake St. Clair. *Journal of Geophysical Research: Oceans*, *94*, 4947–4958.
- Schwab, D. J., & Morton, J. A. (1984). Estimation of overlake wind speed from overland wind speed: A comparison of three methods. *Journal of Great Lakes Research*, *10*(1), 68–72.
- Silva, C. P., Marti, C. L., & Imberger, J. (2014). Horizontal transport, mixing and retention in a large, shallow estuary: Río de la Plata. *Environmental Fluid Mechanics*, *14*, 1173–1197.
- Sterner, R. W., Ostrom, P., Ostrom, N. E., Klump, J. V., Steinman, A. D., Dreelin, E. A., et al. (2017). Grand challenges for research in the Laurentian Great Lakes. *Limnology and Oceanography Methods*, *62*, 2510–2523.